that ΔE accounts virtually quantitatively (after allowing for slight variations in χ_s) for the solvent compositional dependence of the optical electron transfer energy.

Before proceeding further, a significant limitation to eq 6 should be noted. In estimating ΔE from MLCT and LMCT transitions we have neglected to correct for solvent compositional effects upon L, L^-, and L^+ energies of solvation, although such energies (or at least their differences) clearly must contribute to the measured values of E^{LMCT} and E^{MLCT}. For the present system these contributions are small, especially in comparison to those occurring at the $(NH_3)_5Ru$ sites, and the use of eq 6 is justified. Nevertheless, for other systems eq 6 may be less applicable.

The observation of major energetic effects in optical electron transfer reactions has implications for related thermal electron exchanges. Unsymmetrical secondary coordination introduces an energy contribution in E^{MMCT} through ΔE in eq 4. As illustrated by Figure 5 the classical activation barrier (ΔG^*) for the corresponding thermal electron transfer should increase by $\sim 0.5\Delta E$. For $\Delta E = 1300$ cm^{-1}, $\Delta\Delta G^*$ is 1.9 kcal mol^{-1} and the expected influence upon the exchange rate constant is a decrease of about $1^1/_2$ orders of magnitude. We plan to search for such effects in pseudo-self-exchanges like $[(NH_3)_5Ru(nicotinamide)]^{3+}/[(NH_3)_5Ru(isonicotinamide)]^{2+}$. We are also attempting to extend the analysis to reactions that involve a change in *primary* coordination number, like the $Eu_{aq}^{3+/2+}$ self-exchange.

Acknowledgment. This material is based upon work supported by the National Science Foundation through the Presidential Young Investigator Program under Grant No. CHE-8552627 and by the Atlantic Richfield Foundation through a Junior Faculty Fellowship. Helpful discussions with Dr. Jeff Curtis are acknowledged.

Contribution from the Department of Chemistry,
University of San Francisco, San Francisco, California 94117-1080

Redox-State-Dependent Preferential Solvation of Ruthenium(II) and Ruthenium(III) Ammine Complexes. Implications for Electron-Transfer Processes in Mixed Solvents

Kelly S. Ennix, Peter T. McMahon, Roger de la Rosa, and Jeff C. Curtis*

Received February 11, 1987

Preferential solvation of the asymmetric binuclear complex $(bpy)_2Ru^{II}Cl(pyz)Ru^{II/III}(NH_3)_4py^{3+/4+}$ by Me_2SO in acetonitrile has been studied via UV–vis, near-IR, and electrochemical techniques. It is found that the strong donor Me_2SO preferentially solvates the mixed-valence 4+ form of the dimer to a greater degree than the fully reduced 3+ form due to the relatively higher Lewis acidity of the ammine protons when coordinated to Ru(III). As one index of this, the equisolvation point of the II,II dimer is found at $\chi_{Me_2SO} = 0.104$ whereas that for the II,III form is at $\chi_{Me_2SO} = 0.003$. The degree of solvent "re-sorting" that must occur upon a change in redox state at the ruthenium ammine moiety as a function of χ_{Me_2SO} is quantified and found to go through a maximum at $\chi_{Me_2SO} \cong 0.019$. It is concluded that a solvent trapping barrier arising from nonequilibrium preferential solvation must be considered in situations involving electron-transfer processes of preferentially solvated solutes.

The importance of specific solvent–solute interactions in determining the redox thermodynamics and electron-transfer kinetics of transition-metal complexes has received considerable recent attention.[1-4] Investigations in this laboratory have shown that specific interactions of a hydrogen-bonding nature can be predominant in defining the solvent-dependent portion of the Franck–Condon barrier to optical electron transfer in asymmetric mixed-valence dimers such as (1).[5] (bpy = 2,2′-bipyridine, py

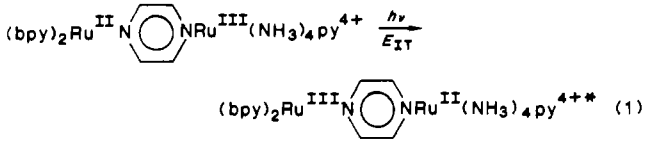

(1)

= pyridine, and E_{IT} denotes the energy of the intervalence-transfer absorption band maximum.) In this case it was found that strong Lewis base solvents (as indicated by large Gutmann donor numbers[6]) interacted with the solute in such a way as to both increase the redox asymmetry in the molecule by stabilizing the ruthenium(III)–ammine form of the dimer relative to the ruthenium(II)–ammine form and also increase the Franck–Condon energy of the transition by essentially adding a new dimension to the multidimensional potential energy surfaces defining it.

In mixed-valence systems where specific interactions with the medium are negligible, it has been amply demonstrated that the solvent-dependent portion of the Franck–Condon energy can be accounted for by using the dielectric continuum theory of nonequilibrium solvent polarization developed by Marcus and Hush.[7-9] This form of solvent-imposed barrier arises from the fact that it is only the very high (optical) frequency portion of the mediums' polarizability that can remain in equilibrium with the rapidly changing charge distribution attending electron-transfer events. On the basis of the geometric approximation for the donor–acceptor pair of two spheres with radii small compared to their center–center distance, the solvent barrier can be expressed as[7-9]

$$\lambda_{outer} = e_0^2\left(\frac{1}{2a_1} + \frac{1}{2a_2} - \frac{1}{d}\right)\left(\frac{1}{n^2} - \frac{1}{D_s}\right) \qquad (2)$$

where e_0 is the electron's charge, a_1 and a_2 are the radii of the sites, n^2 is the optical dielectric constant (square of the refractive index), and D_s is the static dielectric constant.

In this paper we wish to report on investigations carried out on the molecule shown in (1) in solvent mixtures of the moderate-donor-strength solvent acetonitrile (donor number = 14.1) and the high-donor-strength solvent dimethyl sulfoxide, Me_2SO (donor

(1) (a) Gutmann, V. *Electrochim. Acta* **1978**, *21*, 661. (b) Kotocova, A.; Mayer, U. *Collect. Czech. Chem. Commun.* **1980**, *45*, 335. (c) Mayer, U.; Gerger, W.; Gutman, V. *Z. Anorg. Allg. Chem.* **1980**, *464*, 200.
(2) Mascharak, P. K. *Inorg. Chem.* **1986**, *25*, 245.
(3) (a) Hupp, J. T.; Weaver, M. J. *J. Phys. Chem.* **1984**, *88*, 1800. (b) Hupp, J. T.; Weaver, M. J. *J. Phys. Chem.* **1985**, *89*, 1601. (c) Hupp, J. T.; Weaver, M. J. *Inorg. Chem.* **1984**, *23*, 3639.
(4) Lay, P. A. *J. Phys. Chem.* **1986**, *90*, 878.
(5) Chang, J. P.; Fung, E. Y.; Curtis, J. C. *Inorg. Chem.* **1986**, *25*, 4233.
(6) Gutmann, V. *The Donor-Acceptor Approach to Molecular Interactions*; Plenum: New York, 1978.
(7) (a) Marcus, R. A. *J. Chem. Phys.* **1956**, *24*, 906. (b) Marcus, R. A. *Annu. Rev. Phys. Chem.* **1964**, *15*, 155.
(8) (a) Hush, N. S. *Trans. Faraday Soc.* **1961**, *57*, 557. (b) Hush, N. S. *Prog. Inorg. Chem.* **1967**, *8*, 391.
(9) Creutz, C. *Prog. Inorg. Chem.* **1983**, *30*, 1.

0020-1669/87/1326-2660$01.50/0

Table I. Visible Spectral Data for the Lowest Energy MLCT Band of $(bpy)_2Ru^{II}Cl(pyz)Ru^{II}(NH_3)_4py(PF_6)_3$ in Mixtures of Me_2SO/Acetonitrile

χ_{SO}	λ_{max}(MLCT), nm	E_{max}, eV	$\delta m/\delta t$
0.000	553.8 ± 0.3	2.239	0.000
0.005	555.6	2.232	0.097
0.008	556.8	2.227	0.162
0.030	558.1	2.222	0.297
0.100	562.9	2.203	0.487
0.200	567.2	2.186	0.716
0.300	567.8	2.184	0.743
0.400	569.9	2.176	0.851
0.500	570.4	2.174	0.878
0.600	571.7	2.169	0.946
0.800	572.5	2.166	0.986
0.900	572.7	2.165	1.000
1.000	572.7	2.165	1.000

number = 29.8). By studying the degree of preferential solvation of Me_2SO about the ruthenium–ammine end of the dimer as a function of redox state (either fully reduced II,II, or mixed-valence II,III), we have been led to consider the existence of an interesting form of solvent-imposed trapping barrier peculiar to mixed-solvent systems. This barrier involves the degree to which the solvent about the ammine moiety must "re-sort" itself upon a change in redox state and can be aptly described as *nonequilibrium preferential solvation.*

Preferential solvation of a solute by one component of a solvent mixture over another has been extensively investigated by NMR and visible spectroscopies and has been shown to be of primary importance in determining the kinetics of certain solvent substitution processes at transition-metal centers[10] (see also ref 6, Chapter 9). Covington and co-workers have worked out and verified a theory for the process involving a successive coordination model[11] and Remerie and Engberts have recently offered some useful refinements.[12]

To date, relatively little systematic work has been done regarding electron-transfer processes in mixed organic solvents, although we have found reports of some quite interesting results for bimolecular electron-transfer reactions in mixed aqueous/nonaqueous solutions. In many cases the observed rates appear to go through minima at certain solvent compositions.[13] These results may become more understandable in light of the nonequilibrium preferential solvation model to be presented here.

Experimental Section

Materials. $(bpy)_2RuCl(pyz)Ru(NH_3)_4py(PF_6)_3$ was prepared according to the techniques reported in ref 5. Anal. Calcd (found) (two waters of hydration): C, 27.89 (27.84); H, 3.31 (2.98); N, 12.39 (11.82); C/N, 2.25 (2.36).

Solvents were spectrograde and were passed over activated alumina prior to use. The solvent mixtures were made up by weight fractions in sufficient quantity to insure a minimum of two significant figures accuracy in the calculated mole fractions. They were stored over 3-Å molecular sieves in airtight containers. Care was taken to minimize exposure time to the atmosphere during the experiments.

Spectroscopic Measurements. UV–vis–near-IR spectra were recorded on a Perkin-Elmer 330 spectrophotometer with the slits operating under servo control. Room temperature was 20 ± 2 °C.

For the near-IR experiments the mixed-valence $(bpy)_2Ru^{II}Cl(pyz)$-$Ru^{III}(NH_3)_4py^{4+}$ ion was generated by addition of $(bpy)_2Fe^{III}(PF_6)_3$ as oxidant as described in ref 5. The concentration of the II,III dimer was kept at or below 7×10^{-4} M. This was in order to insure that the concentration of complex was always at least 20-fold less than the concentration of Me_2SO even at the lowest χ_{Me_2SO} investigated (0.0010).

Electrochemical Measurements. Differential-pulse polarograms were recorded on an IBM 225ec electrochemical analyzer at a sweep rate of 2 mV/s, pulse amplitude of 5 mV, and drop time of 0.2 s on a freshly polished Pt disk electrode. The supporting electrolyte was 0.10 M tetraethylammonium hexafluorophosphate (also prepared according to ref 5). The instrumental reference was a saturated SCE and the position of the ferrocene/ferrocenium (fc/fc^+) couple at high dilution was used as a quasi-solvent-independent reference.[14]

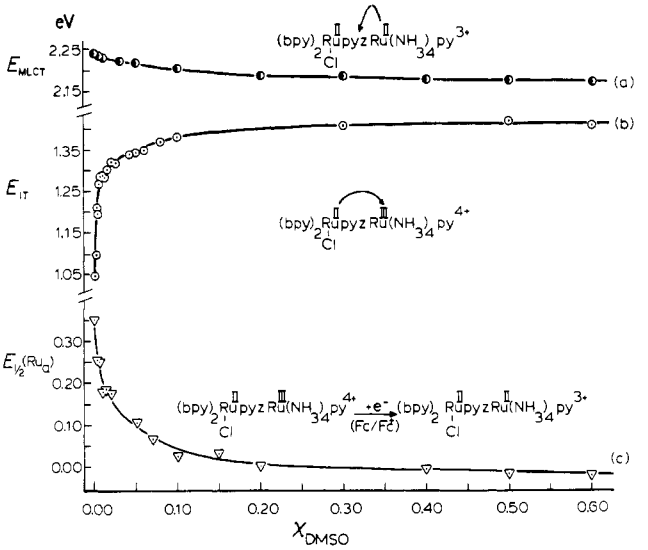

Figure 1. Spectroscopic and electrochemical properties of the dimer $(bpy)_2RuCl(pyz)Ru(NH_3)_4py^{3+/4+}$ as the mole fraction of Me_2SO in acetonitrile is increased: (a) the metal-to-ligand charge-transfer-band maximum of the fully reduced 3+ form; (b) the intervalence-transfer-band maximum of the mixed-valence form; (c) the reduction potential of the ruthenium–ammine end vs. ferrocene/ferrocenium.

Table II. Near-IR Spectral Data for the IT Transition in $(bpy)_2Ru^{II}Cl(pyz)Ru^{III}(NH_3)_5py^{4+}$

χ_{Me_2SO}	λ_{max}(IT), nm	E_{IT}, eV	$\delta m/\delta t$
0.0000	1183 ± 3	1.038 ± 0.005	0.000
0.0010	1127	1.100	0.167
0.025	1022	1.213	0.470
0.0030	1030	1.204	0.446
0.0050	976	1.270	0.623
0.0075	965	1.285	0.664
0.0080	961	1.290	0.677
0.010	963	1.288	0.672
0.015	952	1.303	0.712
0.020	936	1.324	0.769
0.050	921	1.346	0.830
0.060	919	1.350	0.839
0.100	897	1.382	0.925
0.300	879	1.410	1.000
0.500	873	1.420	1.025
0.600	879	1.410	1.000
0.800	880	1.409	0.997
0.900	876	1.415	1.013
1.000	879	1.410	1.000

Results

The spectroscopic data for the lowest lying MLCT transition of the fully reduced dimer in the solvent mixtures are listed in Table I. This band energy falls well below the lowest observed MLCT band (thought to be $d\pi(Ru(II)) \rightarrow \pi^*(pyz)$) in the sym-

(10) (a) Frankel, L. S.; Stengle, T. R.; Langford, C. H. *Chem. Commun.* **1965**, 394. (b) Behrendt, S.; Langford, C. H.; Frankel, L. S. *J. Am. Chem. Soc.* **1969**, *91*, 2236. (c) Frankel, L. S.; Langford, C. H.; Stengle, T. R. *J. Phys. Chem.* **1970**, *74*, 1376. (d) Stengle, T. R.; Pan, Y. E.; Langford, C. H. *J. Am. Chem. Soc.* **1972**, *94*, 9037. (e) Langford, C. H.; Tong, J. P. K. *Acc. Chem. Res.* **1977**, *10*, 258. (f) Langford, C. H.; Tong, J. P. K. *Pure Appl. Chem.* **1977**, *49*, 93.

(11) (a) Covington, A. K.; Newman, K. E. *Adv. Chem. Ser.* **1976**, *No. 155*, 153. (b) Covington, A. K.; Lilly, T. H.; Newman, K. E.; Porthouse, G. A. *J. Chem. Soc., Faraday Trans. 1* **1973**, *69*, 963, 973.

(12) Remerie, K.; Engberts, J. B. F. N. *J. Phys. Chem.* **1983**, *87*, 5449.

(13) (a) Vicenti, M.; Pramauro, E.; Pelizzetti, E. *Transition Met. Chem. (Weinheim, Ger.)* **1985**, *8*, 273. (b) Holba, V.; Harcarova, V.; Tarnovska, M. *Chem. Zvesti* **1983**, *37*, 721. (c) Tan, Z. C. H.; Amis, E. S. *J. Inorg. Nucl. Chem.* **1966**, *28*, 2889. (d) Mayhew, R. T.; Amis, E. S. *J. Phys. Chem.* **1975**, *79*, 862. (e) Micic, O. I.; Cercek, B. *J. Phys. Chem.* **1974**, *78*, 285. (f) Micic, O. I.; Cercek, B. *J. Phys. Chem.* **1977**, *81*, 833.

(14) Sahami, S.; Weaver, M. J. *J. Electroanal. Chem. Interfacial Electrochem.* **1981**, *155*, 171.

Table III. Electrochemical Data for the Dimer $(bpy)_2RuCl(pz)Ru(NH_3)_4py(PF_6)_3$ in Mixtures of Me_2SO/Acetonitrile[a]

χ_{Me_2SO}	$E_{1/2}$(fc/fc$^+$) vs. SCE, V	$E_{1/2}(Ru_a)$ vs. fc/fc$^+$, V	$E_{1/2}(Ru_b)$ vs. fc/fc$^+$, V	$\Delta E_{1/2}$, V	$\delta m/\delta t$	
					$\Delta E_{1/2}$	$E_{1/2}(Ru_a)$
0	0.396	0.351	0.637	0.286	0.00	0.00
0.003	0.390	0.253	0.626	0.373	0.23	0.265
0.005	0.392	0.250	0.636	0.386	0.27	0.273
0.010	0.407	0.180	0.610	0.430	0.38	0.462
0.020	0.395	0.173	0.635	0.462	0.46	0.481
0.050	0.409	0.107	0.619	0.512	0.60	0.659
0.070	0.410	0.067	0.612	0.545	0.68	0.768
0.090	0.407	0.052	0.598	0.546	0.685	0.808
0.100	0.421	0.026	0.605	0.579	0.77	0.878
0.150	0.429	0.034	0.618	0.583	0.78	0.857
0.200	0.430	0.002	0.614	0.612	0.86	0.943
0.400	0.429	−0.004	0.601	0.605	0.84	0.959
0.500	0.434	−0.016	0.634	0.650	0.96	0.992
0.600	0.438	−0.022	0.612	0.634	0.92	1.008
0.900	0.444	−0.022	0.623	0.645	0.95	1.008
1.000	0.433	−0.020	0.630	0.650	1.00	1.000

[a] 0.1 M TEA(PF_6), Pt disk, differential-pulse polarography at 2 mV/s sweep rate, 5 mV pulse amplitude, 0.2 s drop time, and room temperature (20 ± 2 °C).

metrical $[(bpy)_2Ru^{II}Cl]_2pyz^{2+}$ ion, which peaks at 513 nm in pure acetonitrile.[15] It also falls well below the energy of the $d\pi(Ru(II)) \rightarrow \pi^*(py)$ MCLT band in the $(NH_3)_4Ru^{II}py^{2+}$ ion.[16] Thus we are able to assign this band as being largely $d\pi(Ru(II)) \rightarrow \pi^*(pyz)$ in character. Figure 1a shows the correlation obtained between E_{MLCT} and χ_{Me_2SO}. The observed strong positive deviation from the linear correlation which would obtain in the case of a purely statistical solvation sphere indicates preferential solvation by Me_2SO at the ammine end of the molecule (the MLCT bands of Ru(II)–ammine complexes are well-known to fall dramatically in energy with increasing solvent donicity whereas those of polypyridyl–Ru(II) complexes do not[17]). Visually the compound is seen to change from purple to bluish purple with increasing χ_{Me_2SO}.

Table II lists the data obtained for the intervalence-transfer transition shown in (1). Curve b in Figure 1 displays the correlation with mole fraction. In this case the shift in energy is opposite in direction and considerably increased in magnitude compared to that of the MLCT transition. The degree of preferential solvation in this case is also seen to be a much more sharply varying function of χ_{Me_2SO}.

The electrochemical data are listed in Table III and Figure 1c shows the correlation of $E_{1/2}(Ru_a)$ with mole fraction (the redox potential of the ammine end of the molecule vs. fc/fc$^+$). Inspection of Table III shows that the $E_{1/2}(Ru_a)$ potential varies strongly with χ_{Me_2SO} while that for $E_{1/2}(Ru_b)$, the nonspecifically interacting end of the dimer, undergoes only subtle and not particularly systematic shifts. The position of the fc/fc$^+$ couple itself relative to the SCE is found to shift anodically by about 45 mV upon going from pure acetonitrile to pure Me_2SO. This is somewhat less than the 100-mV shift reported by Sahami and Weaver in 0.10 $LiClO_4$ supporting electrolyte.[14]

Discussion

The theory of preferential solvation as developed by Covington leads to (3),[12] where δm is the shift in some measureable quantity

$$\delta m/\delta t = \frac{\sum_{i=1}^{N}(K^{1/N}Y)^i(i/N)k^{i(i-N)/2}\prod_{j=1}^{i}[(N+1-j)/j]}{\{1+\sum_{i=1}^{N}(K^{1/N}Y)^i k^{i(i-N)/2}\prod_{j=1}^{i}[(N+1-j)/j]\}} \quad (3)$$

in a solvent mixture relative to the pure starting solvent and δt is the magnitude of the total shift upon going from pure solvent component 1 to pure component 2. Thus $\delta m/\delta t$ is a measure of the fractional shift in an observable. The assumption is made that this shift is linear in the mole fraction of solvent in the solvation sphere of the solute (n/n_0 in the notation of ref 10). Though this idea is chemically reasonable and has been relied upon in all the work in this field thus far, it should be noted that a means to test it would be very helpful. N is the number of solvent molecules in the solvation sphere (assumed constant), $K^{1/N}$ is the equilibrium constant for preferential solvation such that $\Delta G_{PS} = -NRT \ln K^{1/N}$ for complete solvation sphere exchange, and k is a measure of how each successive solvent molecule replacement reaction influences the thermodynamics for the next (if $k > 1$, the next step will be more favorable).[12] As in the work of Remerie and Engberts we will use the solvent mole fraction, χ_{Me_2SO}, rather than the ratio of activity coefficients as the solvent parameter Y in (3). This introduces an ambiguity into the derived $K^{1/N}$ values since it becomes impossible to judge to what degree the observed preferential solvation results from true "solute preference" for one solvent over another as opposed to preferential solvation driven by solution nonideality effects, which can cause the ratios of activity coefficients to deviate from the mole fractions.

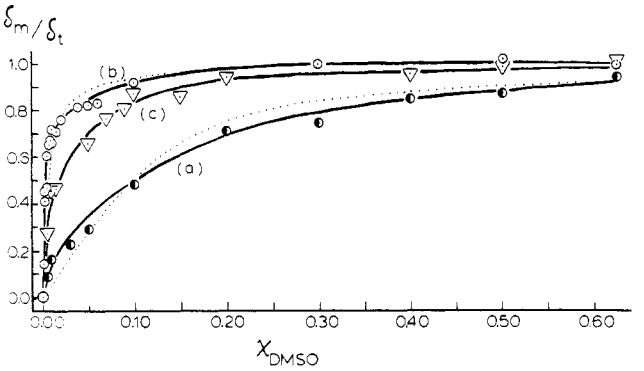

Figure 2. Fractional shifts in the measured quantities of Figure 1 as χ_{Me_2SO} is varied. The dotted lines are the best fits obtainable from eq 3.

Figure 2 shows plots of $\delta m/\delta t$ for the observables of Figure 1 as a function of χ_{Me_2SO}. The solid lines are best-fit curves for the data calculated in a piecewise manner by using a polynomial least-squares method, and the dotted lines are the best fits that could be obtained by using (3). Figure 2a describes the fractional shift in the observable E_{MLCT} as χ_{Me_2SO} is increased, Figure 2b represents E_{IT}, and Figure 2c is for $E_{1/2}(Ru_a)$. The electrochemical $E_{1/2}(Ru_a)$ measurement necessarily reflects the degree of preferential solvation occuring in *both* the oxidized and reduced states. It is in line with intuitive expectations that this curve should lie *between* the other two. A very similar curve is obtained if one plots the difference in potentials $\Delta E_{1/2} = [E_{1/2}(Ru_a) - E_{1/2}(Ru_a)]$ vs. χ_{Me_2SO}.

(15) Callahan, R. W.; Keene, R. F.; Meyer, J. J.; Salmon, D. J. *J. Am. Chem. Soc.* **1977**, *99*, 1064.
(16) Ford, P. C.; Rudd, D. P.; Gaunder, R.; Taube, H. *J. Am. Chem. Soc.* **1968**, *90*, 1187.
(17) Curtis, J. C.; Sullivan, B. P.; Meyer, T. J. *Inorg. Chem.* **1983**, *22*, 224–236.

Table IV. Variations in the Least-Squares-Fitted Parameters for $K^{1/N}$ and k with N

N	$K^{1/N}$	k
For the MLCT Transition (Dotted Curve a, Figure 2)		
8	12 ± 1	1.10 ± 0.03
10	11	1.10
12	11	1.08
For the IT Transition (Dotted Curve b, Figure 2)		
8	180 ± 10	0.90 ± 0.03
10	180	0.90
12	180	0.90

It should be noted that (3) is derived on the assumption of a constant value for N as the solvent composition is varied. Considerable uncertainty is involved in choosing a value for N. Reynolds et al. found an N value of 10 for $Cr^{III}(NH_3)_5(Me_2SO)$ in mixtures of Me_2SO/water.[18] Given the somewhat more hindered nature of the dimer under investigation in this work and the general uncertainty in N, we consider possible solvation numbers from 8 to 12 and list the resulting best-fit values for $K^{1/N}$ and k in Table IV. As the table indicates, the results are quite insensitive to N and it can be concluded that upon going from ruthenium(II) to ruthenium(II) ammine groups the equilibrium constant $K^{1/N}$ goes up by a factor of about 15.6. In terms of the free energy change associated with preferential solvation, this amounts to a change from about −1.5 kcal mol^{-1} (Me_2SO molecule)$^{-1}$ to about −3.1 kcal/mol^{-1} (Me_2SO molecule)$^{-1}$. This difference of −1.6 kcal is an unambiguous quantity since any solution nonideality effects will subtract out.

In spite of the approximate nature of (3), the observed fits are close enough to lend general credence to the theoretical model and to indicate that the derived values of $K^{1/N}$ are reasonable indicators of the strength of the driving force behind preferential solvation. The physical significance of the secondary k parameters, however, is less obvious.

The observed preferential solvation behavior and the redox-state dependence exhibited in Figure 2 derive from the fact that (a) Me_2SO is a significantly stronger Lewis base than acetonitrile (donor number = 29.8 vs. 14.1) and hence is preferentially associated with the acid ammine protons due to stronger hydrogen-bond formation and (b) this sorting effect is amplified by the increase in the acidity of these protons that occurs upon oxidation of the central metal. The dramatic effect of the redox state observed here is not surprising given the known redox-state-dependent Brønsted acidity of other ligands such as H_2O, H_2S, or pyrazinium when bound to ruthenium.[19,20] The results illustrated here, however, do offer a quite striking example of how important a specific solvent–solute interaction can be in defining the nature of second coordination sphere effects.[21]

An alternative index by which to measure the degree of preferential solvation is the "equisolvation point" as originally discussed by Langford et al.[10] This is the point in minority solvent concentration at which $\delta m/\delta t = 0.5$, i.e., where the solute has a 50:50 solvation shell composition. Inspection of Figure 2 shows that this point shifts dramatically from $\chi_{Me_2SO} = 0.104$ for the II,II dimer to about 0.003 for the II,III dimer. In fact, to our knowledge the extremely low value for the II,III dimer is probably the smallest yet observed for any solute.

A third and quite interesting piece of information that can be gleaned from Figure 2 relates to the degree of solvation sphere *reorganization* or *re-sorting* that must necessarily occur when the oxidation state of the ruthenium–ammine moiety is changed. At any given value of χ_{Me_2SO}, the vertical displacement between solid curves a and b of Figure 2 is a measure of this reorganization. There will be a larger percentage of Me_2SO in the solvation sphere about the Ru(III)–ammine complex than in that about the Ru(II)–ammine complex. If this displacement is plotted as a function of χ_{Me_2SO}, Figure 3 is obtained. The curve shows a rapid rise to a broad peak at about $0.019\chi_{Me_2SO}$ followed by a fairly slow tailing off.

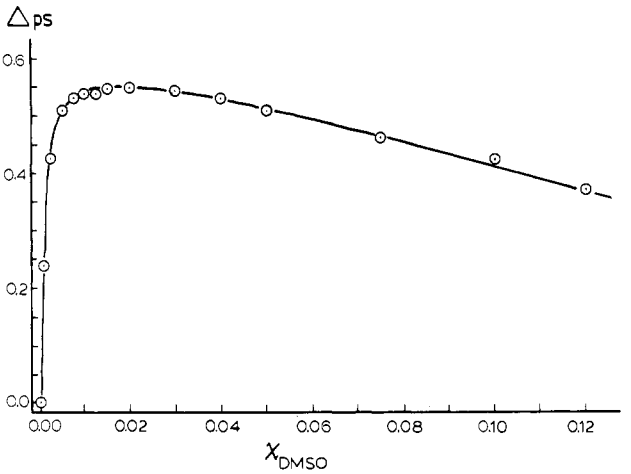

Figure 3. Degree of solvent re-sorting attending a change in redox state of the ruthenium ammine group obtained by subtracting solid curve a of Figure 2 from solid curve b of Figure 2.

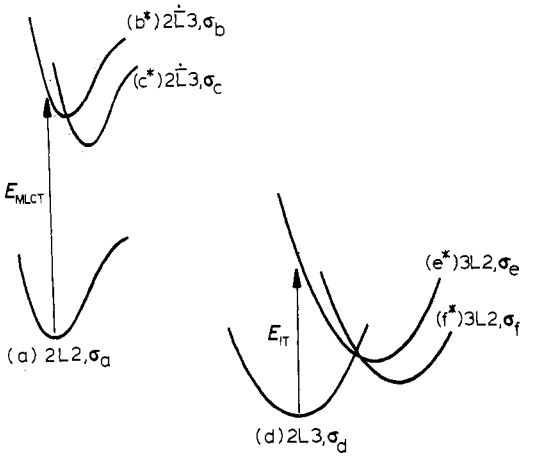

Figure 4. Schematic representation of the potential surfaces governing the MLCT and IT transitions. States b* and e* represent the states of nonequilibrium solvation reached upon a vertical transition from the ground states a and b. States c* and f* represent the resolvated excited states.

One would expect to find the entropy change associated with intramolecular electron transfer or with simple redox at the ammine end to go through an extremum at this value of χ_{Me_2SO} since the solvent "re-sorting" process should have entropic consequences.[22] Similarly, one might expect the kinetics of electron transfer to be influenced by the maximum degree of *nonequilibrium preferential solvation* required to reach the intersection region between the product's and the reactant's potential energy surfaces. This stands as a possible explanation of the rate constant minima observed in the kinetic data reported in ref 13. Relevant to this point, solvent sorting has been identified as an important factor in determining the rates and activational parameters of alkyl halide solvolysis reactions in aqueous/organic mixtures.[23a] Also,

(18) Reynolds, W. L.; Reichley-Yinger, L.; Yaun, Y. *Inorg. Chem.* **1985**, *24*, 4273–4278.
(19) Kuehn, C.; Taube, H. *J. Am. Chem. Soc.* **1976**, *98*, 689.
(20) Taube, H. *Pure Appl. Chem.* **1979**, *51*, 901.
(21) Balzani, V.; Sabbatini, N. *Chem. Rev.* **1986**, *86*, 319–337.
(22) It is known, for example, that large positive entropy changes can accompany the release of electrostricted solvent when the charge density at a metal center is decreased.[3c,25] Because acetonitrile and Me_2SO both have solvent acceptor numbers of 19.3, the acceptor number dependence of $\Delta S°_{rc}$ as identified by Hupp and Weaver will be of little consequence as χ_{Me_2SO} is varied. We thus reason that the maximum $\Delta S°_{rc}$ should occur at the point in χ_{Me_2SO} where the maximum degree of solvent randomization accompanies reduction at the ruthenium–ammine center. Work in progress is designed to probe this idea.[36]
(23) (a) Hyde, J. B. *J. Am. Chem. Soc.* **1960**, *82*, 5129. (b) Blandamer, M. J.; Burgess, J. *Chem. Soc. Rev.* **1975**, *4*, 55.

Scheme I. MLCT and $E_{1/2}(Ru)_a$ Processes

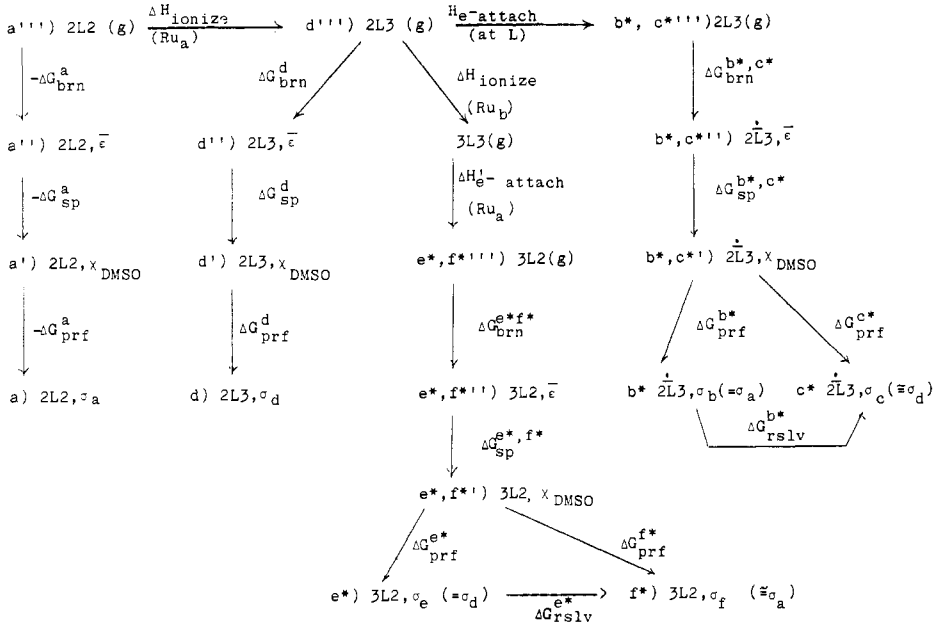

differential dependences of reactant and transition-state chemical potentials as a function of solvent composition have been considered as a possible explanation for the complicated kinetics observed for peroxydisulfate oxidations of Fe(II) complexes.[24]

Implications with Regard to Potential Energy Surfaces. Figure 4 is a schematic representation of the potential energy surfaces that govern the spectroscopic MLCT and IT processes. The notation being used is that state a, labeled as $(2L2,\sigma_a)$, represents the ground-state, fully reduced ion $(bpy)_2Ru^{II}Cl(pyz)Ru^{II}(NH_3)_4py^{3+}$ surrounded by its equilibrium solvent environment σ_a, as defined by the value of $\delta m/\delta t(E_{MLCT})$ at a given χ_{Me_2SO} from Figure 2a. The general variable σ_i can be thought of as the mole fraction of Me_2SO in the solvation sphere as opposed to χ_{Me_2SO}, which refers to the bulk. The subscript i denotes which state is being referred to. The notation for state b*, $(2L^{\bullet-}3,\sigma_b)$, implies the MLCT excited-state $(bpy)_2Ru^{II}Cl(pyz^{\bullet-})Ru^{III}(NH_3)_4py^{3+*}$ in the nonequilibrium solvent environment σ_a of the ground state ($\sigma_b = \sigma_a$). State c* is also an MLCT excited-state ion but is now in its equilibrium solvation environment σ_c.

Whether the initially populated state b* is able to thermally relax to the bottom of its potential well prior to the solvent resorting that carries it to c* is dependent upon the relative rates of these processes. Vibrational relaxation of excited states is generally throught to occur within a few picoseconds after excitation.[26] The diffusional relaxation times to re-sort the solvent about the long-lived excited state of the solute 4-aminophthalimide in 1-propanol/toluene mixtures have been observed to vary from 2.7 ns at low $\chi_{1\text{-propanol}}$ to 170 ps at high $\chi_{1\text{-propanol}}$.[27] These diffusional relaxation times are longer than the dielectric relaxation times of either component or of their mixtures. The viscosities of acetonitrile and Me_2SO are very similar to those propanol and toluene;[28] hence, vibrational relaxation to the bottom of well b* prior to resolvation seems probable.

Another important question concerns the lifetime of the vibrationally relaxed state b*. Recent results obtained by Creutz and co-workers have shown that the longest lived MLCT excited state for a ruthenium–ammine complex at room temperature is found for pentaamine (isonicotinamide)ruthenium(II), which has a lifetime of about 200 ps.[29] The lifetime of the bridge-centered MLCT state under consideration here is probably much shorter due to its lower energy[30] and the known consequences of the energy-gap law on the nonradiative decay rates.[31] If the lifetime of this state is on the order of 20 ps and the diffusional relaxation rate is 0.5 ns., then only a small fraction of the vibrationally relaxed b* states will survive long enough to become totally re-solvated.

A similar set of considerations should apply to the transformation of the initially populated intervalence-transfer excited state (e*) into the diffusionally relaxed state (f*). Unfortunately, so little is known about the photophysics of intervalence-transfer excited states that there is no basis for speculation on this point.

As has been shown by Buhse,[27] molecules with charge-transfer excited states long enough lived to have well-defined chemical properties should be amenable to the investigation of the photophysics of excited-state resolvation. Efforts along these lines using transition-metal complexes are underway in this laboratory.[32]

Solvation Energies and Thermochemical Relationships. The relationships between the various thermodynamic and spectroscopic quantities dealt with thus far and the medium-dependent solvation energies about which they tell us can be understood by considering a thermochemical cycle.

Scheme I illustrates a way in which we can conceptually "de-solvate" the various ground and excited states under consideration so as to isolate the electron-transfer events in the gas phase and thus allow for discussion of the solvent dependences of our experimental observables solely in terms of solvation energies.

The desolvation process invoked here goes in three steps. First the preferential solvation is randomized at an energetic cost of $-\Delta G^i_{prf}$ (where i refers to states a, b*, c*, d, e*, or f*) and the ion's solvation sphere then takes on the same composition as that

(24) (a) Blandamer, M. J.; Burgess, J. *J. Chem. Soc., Chem. Commun.* **1978**, 963. (b) Blandamer, M. J.; Burgess, J.; Duce, P. P.; Haines, R. I. *J. Chem. Soc., Dalton Trans.* **1980**, 2442.
(25) Miralles, A. J.; Armstrong, R. E.; Haim, A. *J. Am. Chem. Soc.* **1977**, *99*, 1416.
(26) Porter, G. B. In *Concepts of Inorganic Photochemistry*; Adamson, A. W., Fleischauer, P. D., Eds.; Wiley: New York, 1975; Chapter 1.
(27) Buhse, L. F. Ph.D. Dissertation, University of California at Berkeley, 1986.
(28) Gordon, A. J.; Ford, R. A. *The Chemists Companion*; Wiley: New York, 1972; Chapter 1.
(29) Winkler, J. R.; Netzel, T. L.; Creutz, C.; Sutin, N. *J. Am. Chem. Soc.* **1987**, *109*, 2381–2392.
(30) The $Ru^{II}(NH_3)_5(isn)^{2+}$ ion exhibits an MLCT absorption maximum at 468 nm in acetonitrile: Kwok, V.; Curtis, J. C., unpublished work.
(31) Kober, E. M.; Caspar, J. V.; Lumpkin, R. S.; Meyer, T. J. *J. Phys. Chem.* **1986**, *90*, 3722–3724 and references therein.
(32) Fung, E. F.; Curtis, J. C., work in progress.
(33) Conway, B. E. *Ionic Hydration in Chemistry and Biophysics*; Elsevier: Amsterdam, 1981; p 237.
(34) Some nonideality in ε̄ as χ_{Me_2SO} is varied might be expected in analogy to what has been found for water–alcohol mixtures. Numerically, however, the consequences with respect to ΔG^i will be small. See: Wyman, J. *J. Am. Chem. Soc.* **1931**, *53*, 3292. Akerlof, G.; Short, O. A. *J. Am. Chem. Soc.* **1936**, *58*, 1241.

of the bulk medium, χ_{Me_2SO}. Second, the energy of specific solvation between the solute and the solvent, ΔG^i_{sp} is surmounted (see ref 3 and 4 for helpful discussions of specific solvation). Third the general, electrostatic Born solvation free energy in a dielectric medium of some average effective dielectric constant $\bar{\epsilon}$, $\Delta G^i_{Born} = ((ze^0)^2/2a)(\epsilon - 1)$, must be overcome. In the Scheme I we start from state a and delineate the pathways to the other states. This scheme thus illustrates the solvation energies relevant to the MLCT (a → b*), one-electron-oxidation (a → d), and IT (d → e*) processes.

In the consideration of a change between thermally equilibrated states such as is measured by the electrochemical $E_{1/2}(Ru_a)$ potential, the free energies of solvation are clearly the relevant quantities. From Scheme I, we can then express the χ_{Me_2SO} dependence of $E_{1/2}(Ru_a)$ as

$$\frac{\partial E_{1/2}(Ru_a)}{\partial \chi_{Me_2SO}} = \frac{\partial}{\partial \chi_{Me_2SO}}(G_d - G_a) = \frac{\partial}{\partial \chi_{Me_2SO}}(\Delta G^d_{prf} + \Delta G^d_{sp} + \Delta G^d_{brn} - \Delta G^a_{prf} - \Delta G^a_{sp} - \Delta G^a_{brn}) \quad (4)$$

The ΔG^i_{sp} and ΔG^i_{brn} solvation energies should vary approximately linearly with χ_{Me_2SO} since they depend only upon the bulk solvent's effective donicity and dielectric constant—neither of which is likely to exhibit drastic nonideality effects. Thus, if the major nonlinear portion of the χ_{Me_2SO} dependency derives from the ΔG^i_{prf} terms, a reasonable first-order approximation to (4) would be

$$\frac{\partial E_{1/2}(Ru_a)}{\partial \chi_{Me_2SO}} = c + \frac{\partial}{\partial \chi_{Me_2SO}}(\Delta G^d_{prf} - \Delta G^a_{prf}) \quad (5)$$

where c is some constant resulting from the ΔG^i_{sp} and ΔG^i_{brn} terms.

In the case of the spectroscopic quantities and their χ_{Me_2SO} dependences, we encounter an important issue with regard to what solvation energies to use in Scheme I—free energies or internal energies (equivalent to enthalpies in the absence of pressure–volume work). Since photons can only affect changes in internal energy, it would initially seem that the various solvation *enthalpies* should be the relevant quantities in deriving expressions analogous to (4) for $\partial E_{MLCT}/\partial \chi_{Me_2SO}$ and $\partial E_{IT}/\partial \chi_{Me_2SO}$. Recent theoretical and experimental work, however, strongly suggests that absorption band energies for charge-transfer processes in fact correlate with the free-energy differences between the initial and final states.[35] Work in progress on the temperature dependences of the same preferential solvation behavior discussed here may be helpful in this regard.[36]

Assuming that the solvation free energies are the appropriate quantities, we then find

$$\frac{\partial E_{MLCT}}{\partial \chi_{Me_2SO}} = c' + (\Delta G^{b*}_{prf} - \Delta G^a_{prf}) \quad (6)$$

and

$$\frac{\partial E_{IT}}{\partial \chi_{Me_2SO}} = c'' + (\Delta G^{e*}_{prf} - \Delta G^d_{prf}) \quad (7)$$

The states reached upon absorption are b* and e* (*vide infra*). Since states b* and e* are not in equilibrium with their solvent environments, we must recognize that ΔG^{b*}_{prf} and ΔG^{e*}_{prf} are not measurable thermodynamic quantities. In combination with the energetics of the excited-state resolvation (re-sorting) processes ΔG^{b*}_{rslv} and ΔG^{e*}_{rslv}, however, they do add up to the thermodynamically calculable ΔG^{c*}_{prf} and ΔG^{f*}_{prf} values.

In a rather more phenomenological approach, we note that the change in energy of any of the initial and final states a → f* with changes in χ_{Me_2SO} can be expressed conveniently if we recognize that its χ_{Me_2SO} dependency is separable into two parts: (a) the actual sensitivity of the state's energy to changes in the fraction of Me_2SO in its solvation sphere, written as $\partial E_i/\partial \sigma_i$; (b) the relationship between the bulk and solvation sphere mole fractions of Me_2SO, written as $\partial \sigma_i/\partial \chi_{Me_2SO}$ (defined experimentally for $\partial \sigma_a/\partial \chi_{Me_2SO}$ and $\partial \sigma_d/\partial \chi_{Me_2SO}$ by the derivatives of curves a and b in Figure 2). Thus we can write eq 8.

$$\partial E_i/\partial \chi_{Me_2SO} = (\partial E_i/\partial \sigma_i)(\partial \sigma_i/\partial \chi_{Me_2SO}) \quad (8)$$

MLCT process; i = a, b*, c*

IT process; i = d, e*, f*

If we consider the chemical natures of the excited states b*, c*, e*, and f*, some useful relationships can be defined. For example, from the standpoint of preferential solvation, the MLCT excited state b* is essentially a ruthenium(III)–ammine complex coordinated to a pyrazine radical-anion bridging ligand. The extent of charge-transfer is thought to amount to 0.8–0.9 electron in such excited states;[37] hence, the ammine protons of b* (or of c*) should have about the same Lewis acidity as those of a ground-state ruthenium(III)–ammine complex. The proximity of the negative charge delocalized over the pyrazine ring should exert only a second-order influence; thus, we hypothesize that the energy of the state (b*) should vary with changes in σ_b ($=\sigma_a$) in approximately the same way as the energy of the ground-state mixed-valence molecule (d)

$$\partial E_{b*}/\partial \sigma \cong \partial E_d/\partial \sigma \quad (9)$$

where the subscripts on σ have been dropped for simplicity. Similarly

$$\partial E_{c*}/\partial \sigma \cong \partial E_d/\partial \sigma \quad (10)$$

Noting the chemical similarities at the ruthenium–ammine site among states a, e*, and f*, we also assert the following:

$$\partial E_{e*}/\partial \sigma^* \cong \partial E_a/\partial \sigma \quad (11)$$

$$\partial E_{f*}/\partial \sigma^* \cong \partial E_a/\partial \sigma \quad (12)$$

Another set of approximate equalities that follows from the preceding chemical arguments involves the actual degree of preferential solvation about the thermally equilibrated states c* and f*

$$\partial \sigma_c/\partial \chi_{Me_2SO} \cong \partial \sigma_d/\partial \chi_{Me_2SO} \quad (13)$$

$$\partial \sigma_f/\partial \sigma_{Me_2SO} \cong \partial \sigma_a/\partial \chi_{Me_2SO} \quad (14)$$

Here the subscripts on σ are important since they tell us which state-specific preferential solvation behavior is being referred to—that of a ruthenium(III)—ammine moiety or that of a ruthenium(II)—ammine moiety.

Having defined these relationships allows us to consider the observed χ_{Me_2SO} dependencies of E_{MLCT}, E_{IT}, and $E_{1/2}(Ru_a)$ in a detailed manner. If we follow the assumption that the states reached upon photon absorption are b* and e*, then (8) allows us to solve for the two spectroscopic quantities

$$\partial E_{MLCT}/\partial \chi_{Me_2SO} = \partial(E_{b*} - E_a)/\partial \chi_{Me_2SO} = (\partial E_{b*}/\partial \sigma)(\partial \sigma_a/\partial \chi_{Me_2SO}) - (\partial E_a/\partial \sigma)(\partial \sigma_a/\partial \chi_{Me_2SO}) \quad (15)$$

$$\partial E_{IT}/\partial \chi_{Me_2SO} = \partial(E_{e*} - E_d)/\partial \chi_{Me_2SO} = (\partial E_{e*}/\partial \sigma)(\partial \sigma_d/\partial \chi_{Me_2SO}) - (\partial E_d/\partial \sigma)(\partial \sigma_d/\partial \chi_{Me_2SO}) \quad (16)$$

For the electrochemical quantity we find

$$\partial E_{1/2}/\partial \chi_{Me_2SO} = \partial(G_d - G_a)/\partial \chi_{Me_2SO} = (\partial G_d/\partial \sigma)(\partial \sigma_d/\partial \chi_{Me_2SO}) - (\partial G_a/\partial \sigma)(\partial \sigma_a/\partial \chi_{Me_2SO}) \quad (17)$$

Applying (9) and (11) to (15) and (16) leads to the following approximations:

$$\partial E_{MLCT}/\partial \chi_{Me_2SO} \cong (\partial E_d/\partial \sigma - \partial E_a/\partial \sigma)(\partial \sigma_a/\partial \chi_{Me_2SO}) \quad (18)$$

$$\partial E_{IT}/\partial \chi_{Me_2SO} \cong (\partial E_a/\partial \sigma - \partial E_d/\partial \sigma)(\partial \sigma_d/\partial \chi_{Me_2SO}) \quad (19)$$

(35) (a) Marcus, R. A.; Sutin, N. *Comments Inorg. Chem.* **1986**, *5*, 119. (b) Haim, A. *Ibid.* **1985**, *4*, 113. (c) Brunschwig, B. S.; Ehrenson, S.; Sutin, N. *J. Phys. Chem.* **1986**, *90*, 3657. (d) Kjaer, A. M.; Kristjansson, I.; Ulstrup, J. *J. Electroanal. Chem. Interfacial Electrochem.* **1986**, *204*, 45. (e) Hupp, J. T., private communication. (f) Kober, E. M., private communication.

(36) Ennix, K.; Curtis, J. C., work in progress.

(37) Zwickel, A. M.; Creutz, C. *Inorg. Chem.* **1971**, *10*, 2395.

Table V. $\partial E_d/\partial\sigma - \partial E_a/\partial\sigma$ As Calculated from (21) at Various Values of χ_{Me_2SO}

χ_{Me_2SO}	$\partial E_{MLCT}/\partial\chi_{Me_2SO}$	$\partial\sigma_a/\partial\chi_{Me_2SO}$	$\partial E_{IT}/\partial\chi_{Me_2SO}$	$\partial\sigma_d/\partial\chi_{Me_2SO}$	$\partial E_d/\partial\sigma - \partial E_a/\partial\sigma$
0	−0.640	18.62	90.62	225	−0.380
0.0025	−0.625	17.50	30.26	115	−0.233
0.0050	−0.612	14.56	9.52	30.0	−0.227
0.0080	−0.566	13.06	5.46	11.5	−0.245
0.0100	−0.545	8.50	3.12	8.40	−0.217
0.025	−0.478	5.10	2.04	4.60	−0.260
0.040	−0.402	4.20	1.22	2.36	−0.256
0.505	−0.442	3.65	0.912	2.06	−0.237
0.080	−0.290	2.92	0.553	1.26	−0.202
0.100	−0.255	2.60	0.431	1.10	−0.185
0.120	−0.195	2.30	0.362	0.84	−0.177
0.150	−0.150	1.88	0.251	0.44	−0.173
0.200	−0.098	1.34	0.102	0.37	−0.117
0.250	−0.007	0.82	0.038	0.135	−0.110
0.300	−0.044	0.70	0.024	0.067	−0.089
0.400	−0.038	0.38	0.016	0.033	−0.131
0.500	−0.025	0.32	0.011	0.018	−0.107
0.600	−0.013	0.14	0.006	0.003	−0.133

[a] $\partial E_{MLCT}/\partial\chi_{Me_2SO}$, $\partial\sigma_a/\partial\chi_{Me_2SO}$, $\partial E_{IT}/\partial\chi_{Me_2SO}$, and $\partial\sigma_d/\partial\chi_{Me_2SO}$ calculated from analytical fits of the curves in Figures 1 and 2.

Since a ruthenium(III)–ammine complex will be stabilized by a given amount of Me_2SO in its solvation shell *more* than the corresponding ruthenium(II) complex, $\partial E_d/\partial\sigma$ will be a larger negative quantity than $\partial E_a/\partial\sigma$; hence, (18) tells us that $\partial E_{MLCT}/\partial\chi_{Me_2SO}$ will be a negative quantity—as is observed experimentally. By analogous reasoning $\partial E_{IT}/\partial\chi_{Me_2SO}$ should be a positive quantity.

Subtracting (19) from (18) and rearranging give the following:

$$\partial E_d/\partial\sigma - \partial E_a/\partial\sigma \cong (\partial E_{MLCT}/\partial\chi_{Me_2SO} - \partial E_{IT}/\partial\chi_{Me_2SO})/(\partial\sigma_a/\partial\chi_{Me_2SO} + \partial\sigma_d/\partial\chi_{Me_2SO}) \quad (20)$$

The prediction here is that, within the accuracy of the assumptions and approximations made in arriving at (20), the quantity on the left-hand side should be constant and negative as χ_{Me_2SO} is varied. Since all the quantities on the right-hand side can be evaluated from the analytical expressions for the slopes of the curves in Figures 1 and 2 at various χ_{Me_2SO}, we are able to test this. Table V shows that the prediction is quite well adhered to at bulk mole fractions greather than about 0.0025 although there does appear to be a slow tailing off. The discrepancy at low χ_{Me_2SO} could be due to nonconstancy in one or both of the $\partial E_i/\partial\sigma$ functions or possibly to the rather large experimental uncertainties in the steep slopes of the curves in Figure 2 at low χ_{Me_2SO}.

Concluding Remarks

The preferential solvation behavior of ruthenium–ammine groups exhibits a sensitive dependence on the redox state of the metal. The observed functional dependencies of the spectroscopic MLCT and IT processes can be reasonably well described by Covington's model.

By factoring the preferential solvation phenomenon into components as detailed in (8) and noting the complementarity that exists between the chemical natures of the ground and excited states relevant to the MLCT and IT processes, we have been able to experimentally probe some rather unique relationships regarding the dependencies of state energies on solvation-sphere composition. The reasonable success of (20) can be taken as evidence that states b* and e* are indeed the appropriate ones to consider in treating the energetics of the two absorption processes. Furthermore, the results allow us to identify the resolvated states c* and f* as "nonspectroscopic" second-coordination-sphere configurations as recently discussed by Balzani[21] (at least in the absorptive sense).

Considerable theoretical[38] and experimental[39] attention has focused recently on the importance of the dynamics of solvent fluctuations in determining the rate at which thermal electron-transfer reactions can be activated. In any situation where the degree of preferential solvation about a solute in a mixed solvent varies strongly with redox state, we expect that the lowest energy pathway from reactants to products along an electron-transfer reaction coordinate will require a nonequilibrium preferential solvation configuration analogous to the nonequilibrium solvent dielectric polarization required in a pure solvent.

This effect probably contributes to the frequently observed rate constant and activational parameter extrema (almost exclusively minima for the former) observed for electron-transfer and solvolysis reactions in mixed aqueous/organic systems.[13,23,24]

Most of the reactions studied thus far, however, are not conclusive in this regard. The competing solvents also serve as labile inner-sphere ligands in some of the electron-transfer reactions studied, and hence subtle effects arising in the solvation sphere will be obscured.[13c-f] Similar considerations apply to the alkyl halide and related solvolysis reactions. In all cases H_2O is the nucleophile, and the leaving group will in general be preferentially solvated by H_2O. Unambiguous determination of the points along the reaction coordinate at which the solvent re-sorting process exerts its influence awaits further work.

In addition to the above mentioned complications, a strongly hydrogen-bonded solvent such as water will undergo substantial changes in solution structure as an organic component is gradually introduced. Composition-dependent solution structural phenomena are no doubt involved in the behavior reported in aqueous/organic solvent mixtures. This aspect of the problem has been discussed by Engberts.[40]

Non-hydrogen-bonded solvent mixtures and substitutionally inert transition-metal complexes with well-defined preferential solvation behaviors such as the system discussed in this work present an attractive means by which to experimentally address the issue of nonequilibrium preferential solvation in electron-transfer processes.

Acknowledgment. The authors wish to express thanks to the Research Corp. for generous support of this work.

Registry No. $(bpy)_2RuCl(pyz)Ru(NH_3)_4py(PF_6)_3$, 99034-74-9; $(bpy)_2Ru^{II}Cl(pyz)Ru^{III}(NH_3)_4py^{4+}$, 99034-91-0; Me_2SO, 67-68-5; acetonitrile, 75-05-8.

(38) Newton, M. D.; Sutin, N. *Annu. Rev. Phys. Chem.* **1985**, *36*, 573. Hynes, J. T. *J. Stat. Phys.* **1986**, *42*, 149. Calet, D. F.; Wolynes, P. G. *J. Phys. Chem.* **1983**, *87*, 3387. Calet, D. F.; Wolynes, P. G. *J. Chem. Phys.* **1983**, *78*, 470.

(39) (a) Gennet, T.; Milner, D. F.; Weaver, M. J. *J. Phys. Chem.* **1985**, *89*, 2787. (b) Huppert, D.; Kosower, E. M. *Chem. Phys. Lett.* **1983**, *96*, 433. (c) Harrer, W.; Grampp, G.; Janicke, W. *Chem. Phys. Lett.* **1984**, *12*, 263. (d) Kapturkiewicz, A.; Behr, B. *J. Electroanal. Chem. Interfacial Electrochem.* **1984**, *179*, 187.

(40) (a) Menninga, L.; Engberts, J. B. F. N. *J. Phys. Chem.* **1978**, *77*, 1271. (b) Engbersen, J. F. J.; Engberts, J. B. F. N. *J. Am. Chem. Soc.* **1974**, *96*, 1231.